US-FT/9-00

Measuring the BFKL Pomeron in Neutrino Telescopes

J.A. Castro Pena, G. Parente and E. Zas

Departamento de Física de Partículas
Universidade de Santiago de Compostela
15706 Santiago de Compostela, Spain

Abstract

We present a new method for obtaining information on the small x behavior of the structure function F_2 outside the kinematic range of present acelerators from the mean inelasticity parameter in UHE neutrino-nucleon DIS interactions which could be measured in neutrino telescopes.

1 Introduction

A variety of models have been proposed in which astrophysical neutrinos exceed the expected atmospheric neutrino flux at energies in the TeV scale or higher [1]. The detectors presently in design or construction stages [2] look for Čerenkov light from the neutrino-induced muon in deep inelastic scattering (DIS) charged current (CC) interactions and take advantage of both the long muon range and the rise of the neutrino cross section to meet the neutrino detection challenge.

Several alternatives have been proposed for observing high energy neutrinos and they are all based on the detection of the showers that are also produced in most of the neutrino interactions. These include the detection of particle shower fronts in the atmosphere in the horizontal direction (Horizontal Air Showers) [3] and coherent pulses from showers in different media, both acoustic [4] and in radio [4, 5] waves. Shower detection is sensitive both to neutral current interactions and to all neutrino flavors. In DIS interactions with nuclei, showers of hadronic type are always initiated by the debris of the struck nucleons. For electron neutrino charged current interactions an electromagnetic shower is initiated at the lepton vertex in addition to the hadronic shower. Certainly conventional detectors in construction can also look for the Čerenkov light from the induced showers provided they are contained or sufficiently close to the instrumented volume. In fact it is likely that shower detection is the main way these detectors can observe ultra high energy neutrinos because of the earth's opacity and the atmospheric muon background.

The high energy neutrino cross section is a crucial ingredient in the calculation of the event rate in high energy neutrino telescopes. The DIS cross section is given in terms of structure functions whose energy dependence (scaling violations) is calculated in perturbative QCD. In practice, structure functions are computed from available parton (quark and gluon) distribution functions which depend on x and Q^2 (see below). Parton densities are extracted from data using DGLAP evolution equations [6] which effectively sum $\ln(Q^2)$ terms contained in the QCD perturbative expansion.

The DGLAP approach can break down at low x because of potentially large $\ln(1/x)$ terms which also appear in the perturbative series. The theoretical behaviour of structure functions at small x has been discussed since the seventies and recently revived in the context of the low x HERA data (see Ref. [7] for a review).

The sumation of the $\ln(1/x)$ terms for intermediate Q^2 is performed with the BFKL formalism [8] which evolves parton densities unintegrated in transverse momentum. Within BFKL at LO and fixed α_s, the structure function F_2 behaves as power like $x^{-\lambda}$, with $\lambda \simeq 0.53$ for α_s=0.2 (for $\alpha_s(M_z^2)$=0.12, $\lambda \simeq 0.32$). The exponent λ is related to the intercept of the Pomeron which governs the high-energy asymptotics of the total cross section. The consideration of NLO effects in BFKL is a matter of present discussion due to the large correction found (λ becames negative). However, recently it has been found [9] that the NLO value of λ, improved by optimization of the renormalization scale, has a very weak dependence on the virtuality Q^2, ranging the values $\lambda \simeq 0.13-0.18$ at $Q^2 = 1-100$ GeV^2.

This result, $x^{-\lambda}$, is obtained in DGLAP when the input structure function at fixed Q_0^2 has a singular behavior at low x but also when it is flat. In the latter case, the solution is the so call double logarithmic approximation (DLA) and effectively resums terms of type $\alpha_s \ln(1/x) \ln(Q^2)$ [10]. After evolution over a suficiently large Q^2 interval, the DLA result mimics the BFKL behavior, $x^{-\lambda}$ [11].

At this point it should be stressed that the low x behavior of structure functions is fundamental in the high energy limit of the neutrino-nucleon DIS cross section. The calculation of the neutrino-nucleon cross section involves an integration over x which corresponds to the fraction of momentum carried by the struck parton (see below). For $x^{-\lambda}$ with $\lambda > 0$, as the neutrino energy increases, the integral becomes dominated by the interaction with partons of lower x, while the Q^2 integral remains dominated by Q^2 values up to the electroweak boson mass squared (see for example [12] and below). For Q^2 above M_W^2 the integrand behaves as Q^{-4} and quickly becomes irrelevant.

On the experimental side there are however no F_2 measurements at very small x and large Q^2. Consequently, in the process of the total cross section calculation, the parton densities extracted from present data must be carefully extrapolated to the region in the x, Q^2 plane without experimenta support. The dominant kinematical region calls for the connection between the low x behavior at intermediate Q^2 (the BFKL region) and the high Q^2 region but at moderate low x obtained in fits to experimental data (the DGLAP region) [16].

The consideration of QCD effects in the neutrino DIS cross section for neutrino energies well above the electroweak boson threshold was done at the end of the seventies [13, 14] motivated by the DUMAND project. Previously the neutrino-nucleon DIS cross section had been studied in detail for lower neutrino energies in an attempt to disentangle asymptotic freedom effects and, in particular, scaling violations (see [15] for a review). The study of the uncertainty in the cross section calculation, which is important in the context of high energy neutrino telescopes, has been recently addressed [17, 18, 19]. The uncertainty due to the extrapolation to high Q^2 is not expected to be large because the low x shape of the parton distribution functions at low Q^2 is narrowly constrained by HERA while the further evolution to high Q^2 values seems well defined by DGLAP QCD evolution. At the highest energies uncertainties within 20% [17], 40% [19] and a factor $2^{\pm 1}$ [18] are typically reported. However we think that the consideration of conventional DGLAP evolution to small x values and high Q^2, as for example $x = 10^{-9}$ and $Q^2 = 10^4$ GeV^2, should at least be questioned in view of absence of data.

Conversely if any neutrino interactions measurements could be made leading to information on the cross section, such information would be of great value to constrain the theoretical predictions at low x and high Q^2. Of particular interest is the y distribution which can be shown very sensitive to the value of λ (see below), y being the fraction of the neutrino energy which flows to the hadronic part of the interaction in the laboratory frame.

This distribution is incidentally very important for neutrino detection, particularly for all the alternatives in neutrino detection which rely on detecting the high energy showers which are always produced at the hadronic vertex, whatever the neutrino flavor and for both charged current (CC) and neutral current (NC) interactions.

The article is organized as follows: Firstly we collect the most relevant formulae used in the calculation of the neutrino nucleon cross section. Then, we present the result for the total cross section and the average inelasticity $\langle y \rangle$ computed from two sets of parton distribution functions. We explain the characteristics of the results for neutrinos, antineutrinos in CC and NC interactions in terms of the parton distribution dependences, stressing the connection between these quantities and the low x limit of the structure functions at the highest energies.

In the assumption that the low x behavior of F_2 at large Q^2 can be described by $x^{-\lambda}$, we present a very simple analytical relation between λ and the average inelasticity $\langle y \rangle$ which does not depend of any other parameter. We suggest that λ could be determined from y-measurements in the events which are expected in high energy neutrino detectors. Although y-measurements could be thought to be rather speculative at this early stage neutrino astronomy is at present, we point out a method to measure y in neutrino telescopes.

2 The neutrino-nucleon DIS cross section at UHE

In terms of structure functions the charged-current (CC) neutrino-nucleon DIS differential cross section is given by:

$$\frac{d\sigma^{\nu(\overline{\nu})N}}{dxdy} = \left(\frac{G_F^2}{4\pi}\right) 2ME_\nu \left(\frac{M_W^2}{M_W^2+Q^2}\right)^2 \left(y_+F_2 - y^2F_L \pm y_-xF_3\right) \tag{1}$$

where $y_\pm = 1 \pm (1-y)^2$, M is the nucleon mass, E_ν the neutrino energy in the lab frame, $Q^2 = 2ME_\nu xy$ and we have neglected terms suppressed by powers of M^2/Q^2.

In the QCD improved parton model, the structure functions F_i ($i = 2, 3, L$) are calculated in terms of quark and gluon distribution functions. At leading order (LO) approximation in perturbative QCD F_2 (xF_3) is simply related to the sum (difference) of parton densities. At next-to-leading order (NLO) further integrals are involved relating at order $\alpha_s(Q^2)$ the parton densities with the structure function. The contribution due to F_L, which is also proportional to $\alpha_s(Q^2)$ becomes small at large Q^2 and like the M^2/Q^2 terms are neglected in this work.

We present, for simplicity, the expressions which relate the cross sections and the parton densities at the LO approximation. Within the above approximations the differential cross section for the charged current (CC) interaction of neutrinos on isoscalar target takes the form:

$$\begin{aligned}
\frac{d^2\sigma^{\nu N}}{dxdy} &= \frac{G_F^2}{\pi}\frac{M_W^4 ME_\nu}{(M_W^2+Q^2)^2}\left[A(x,Q^2) + \overline{B}(x,Q^2)(1-y)^2\right] \\
\frac{d^2\sigma^{\bar{\nu} N}}{dxdy} &= \frac{G_F^2}{\pi}\frac{M_W^4 ME_\nu}{(M_W^2+Q^2)^2}\left[\overline{A}(x,Q^2) + B(x,Q^2)(1-y)^2\right]
\end{aligned} \tag{2}$$

where

$$A(x, Q^2) = x(u + d + 2s + 2b) \;, \quad B(x, Q^2) = x(u + d + 2c + 2t)$$

The antiquark combinations $\overline{A}$ and $\overline{B}$ are obtained from A and B replacing each quark by the corresponding antiquark of the same flavor.

The total cross section is calculated by integration of Eq. (2). We have used two representative sets of parton densities[1]: the LO set from Ref. [21] (MRST98) and the NLO set in the DIS factorization scheme from Ref. [22] (GRV98)[2]. In the integration we extrapolate the quark distribution functions in x below the low x limit given by the authors ($x = 10^{-5}$ for MRST98 set and $x = 10^{-9}$ for the GRV98 set) using the x slope at the lowest x value of the parametrization for each value of Q^2. This simple phenomenological extrapolation agrees with the more elaborated prescriptions based on perturbative QCD as for example the double-logarithmic-approximation which explain HERA data (see [12] and also Fig. 1b). We choose this ad hoc extrapolation for simplicity because our purpose is just to show the sensitivity of the high energy neutrino cross section to the low x parton behavior.

The total charged and neutral current interaction cross sections[3] for both neutrinos and anti-neutrinos calculated with MRST98 partons are shown in Fig. 1a as a function of the neutrino energy. At low energy one can observe the linear rise of the cross section with the neutrino energy (E_ν). At high energy it would follow a logarithmic rise $\ln(E_\nu)$ were it not for the increase of the sea quark densities at small x ($\sim x^{-\lambda}$) which imply a high energy cross section that rises as $(E_\nu)^\lambda \ \ln(E_\nu)$ for E_ν above 1 PeV.

We have also calculated the cross sections with GRV98 partons. For neutrino energies considered in this work, i.e. below 10^{13} GeV, the results are insensitive to the extrapolation below $x = 10^{-9}$. The cross sections from MRST98 and GRV98 parton distribution can be compared in Fig.1b.

[1] The consideration of nuclear effects in parton distributions which could be relevant for heavy nuclei will be presented elsewhere [20]

[2] Rigurously, NLO corrections modify Eq. (2) in the DIS scheme by terms proportional to α_s coming from xF_3. We neglect them in this calculation

[3] For brevity, in this work we do not present the explicit expressions used in the calculation of the NC cross sections

3 The mean inelasticity at UHE

In this work we are interested in the fraction of the neutrino energy which flows to the hadronic part of the interaction in the laboratory frame, y, which is also called inelasticity. For a given muon neutrino high energy flux, this parameter fixes the relative rates of the two main types of detections, using muons in charged current interactions and using the showers produced in the interactions. It is also reponsible for the relative sizes of the electromagnetic and hadronic showers induced in charged current electron neutrino interactions. This quantity is necessary for any attempt at extracting the neutrino energy in high energy neutrino telescopes whether by detecting the shower produced in the interaction or by detecting the muon produced by muon neutrino CC interactions from the detected hadronic shower or muon.

The average value of y can be obtained by integration of the differential cross section:

$$\langle y \rangle = \frac{1}{\sigma} \int_0^1 dy\, y\, \frac{d\sigma}{dy} \tag{3}$$

The energy dependence of $\langle y \rangle$ has been studied in the past to test asymptotic freedom in strong interactions (see [15] for a review). The effect of the boson propagator on the y distribution and the relevance of the small x region were pointed out in Refs. [13, 14].

In the present work we have calculated $\langle y \rangle$ using modern parton densities which better describe the low x kinematic region. The results using MRST98 partons are shown in Fig. 2a.

Let us explain the general features observed in Fig. 2a from the cross section formulas given in Eq. (2). At low energy, the value of $\langle y \rangle$ for ν is larger than for $\bar{\nu}$ because the most important contribution comes from the valence quarks which are suppressed by $(1-y)^2$ in the anti-neutrino cross section formula (see Eq. (2)). If there were not sea quarks, the y distributions given by Eq. (2) would behave as $(1-y)^2$ (would be flat) for antineutrinos (neutrino) and correspondingly $\langle y \rangle = 0.25$ (0.5). In the case of low energy $\bar{\nu}$, the increase of $\langle y \rangle$ with energy is due to the rise of the sea quark distribution functions. For neutrinos, this effect is less apparent.

The depletion of $\langle y \rangle$ for energies above 1000 GeV (see Fig. 2a) is due to the W propagator appearing in Eq. (2) which acts as a cutoff in the integration restricting the values of Q^2 to around M_W^2, i.e. $xy \sim M_W^2/(2ME_\nu)$. Thus, the $d\sigma/dy$ distribution is shifted to lower values of y.

At the highest energies, because of the sea quark dominance, both neutrino and antineutrino cross sections become almost equal (see Fig. 2a) and the small difference between CC and NC interactions is due to the characteristic couplings of the electroweak interaction.

Concerning the value of $\langle y \rangle$, Fig. 2a shows that it typically becomes stable at values slightly above 0.2. It is remarkable that in the high energy limit $\langle y \rangle$ should be constant while the average value of the Bjorken x variable, $\langle x \rangle$, decreases strongly (see Fig. 4b). The low x rise of the sea quark densities (predicted by perturbative QCD) shifts the weight of the cross section to small x values compensating the y distribution.

The energy dependence of $\langle y \rangle$ at high energy is related to the behavior of the slope assumed constant in the extrapolation of the MRST98 quarks at low x. If λ were negative or zero, $\langle y \rangle$ would send to zero in this limit.

For example, if in the cross section calculation one uses GRV98 partons, $\langle y \rangle$ is not constant and we find that it decreases with increasing energy (see Fig. 2b) which reflects the depletion of the effective slope λ of the GRV98 partons with increasing Q^2.

In the following we show that the observed correlation between $\langle y \rangle$ at high energy and λ at low x can be put in analytic form using very simple approximations.

4 Low x physics and high energy neutrino telescopes

Let us assume that F_2 at low x and high Q^2 is given by the power-like expression $F_2 = A(Q^2)\, x^{-\lambda}$, where λ is assumed constant (or smoothly dependent on Q^2 as predicted by [9]) Then the CC neutrino-nucleon differential cross section (in y and Q^2) takes the form:

$$\frac{d^2\sigma}{dydQ^2} = \left(\frac{G_F^2}{4\pi}\right)\left(\frac{M_W^2}{M_W^2+Q^2}\right)^2 A(Q^2)\left(\frac{2ME}{Q^2}\right)^\lambda \frac{[1+(1-y)^2]}{y}\, y^\lambda \tag{4}$$

where in Eq. (1) we have neglected the contribution from F_L and xF_3 structure functions, expected to be negligable at low x and high Q^2.

In the calculation of $\langle y \rangle$ by Eq. (3) the Q^2 integral of Eq. (4) in numerator and denominator cancels at high energy, i.e. provided that $2ME_\nu$ is much larger than M_W^2.

Then one has:

$$\langle y\rangle = \frac{\int_0^1 dy\; y\; \frac{d\sigma}{dy}}{\int_0^1 dy\; \frac{d\sigma}{dy}} \simeq \frac{\int_0^1 dy\; [1+(1-y)^2]\; y^{\lambda}}{\int_0^1 dy\; [1+(1-y)^2]\; y^{\lambda-1}} \tag{5}$$

which can be easily integrated to get the simple analytical relation:

$$\langle y\rangle \simeq \frac{\lambda^3+5\lambda^2+8\lambda}{\lambda^3+6\lambda^2+13\lambda+12} \tag{6}$$

Analogously, one can proceed as above in the calculation of the average Q^2 which is expected (see above) to be around M_W^2 at energies sufficiently above the W propagator threshold. One finds:

$$\langle Q^2\rangle = \frac{1}{\sigma}\int dQ^2\; Q^2\; \frac{d\sigma}{dQ^2} \simeq \frac{1-\lambda}{\lambda} M_W^2 \tag{7}$$

To check Eq. (6), let us find out the value of λ which corresponds to $\langle y\rangle = 0.23$, which is the result from the explicit integration of the CC neutrino-nucleon differential cross section $d\sigma/dy$ calculated with MRST98 parton densities at $E_\nu = 10^{10}$ GeV (see Fig. 2a). Looking at Fig. 3 one finds $\lambda = 0.42$. We have checked that the MRST98 sea partons at $x = 10^{-5}$ and $Q^2 = 10^4$ GeV^2 have this slope which confirms the validity of Eq. (6).

Furthermore , substituting $\lambda = 0.42$ in Eq. (7), one obtains $\langle Q^2\rangle = 0.9\ 10^4$ GeV^2 which agrees with the asymptotic value reached at high energy from explicit numerical integration of the diferential cross section using the MRST98 partons (see Fig. 4a).

Assuming that the mean inelasticity $\langle y\rangle$ could be experimentally determined, Eq. (6) can be inverted to obtain directly the F_2 slope parameter λ at small x for Q^2 around M_W^2, which is outside the kinematic limits of present accelerators.

We have to stress that the measurement of $\langle y\rangle$ will not be easy to obtain because it would require the determination of the final state energy corresponding to both, the nuclear cascade and the lepton. If electron neutrinos are detected, the showers that come out of charged current interactions will have a different character depending on y because the neutrino induced electromagnetic (hadronic) shower arising at the leptonic (hadronic) vertex carries a fraction $1-y$ (y) of the neutrino energy. In particular it has been recently suggested that it may be possible to measure y by using the radio technique [5]. This tecnique relies of the detection of coherent radio pulses from the excess charge in the induced showers in a dense medium such as ice. As the radiation is coherent the angular structure of the distribution is sensitive to the longitudinal development of the shower. The sensitivity to y arises from the elongation of the showers that develop at the electron vertex because of the Landau-Pomerančuck-Migdal (LPM) [24] effect [5].

For the case of muon neutrinos in charged current interactions, both the muon and the nuclear shower in the final state would have to be detected. As the muon energy loss is proportional to the muon energy above 1 TeV, this may not be out of question in a future large conventional neutrino telescope such as IceCube [23] although many difficulties can be forseen. In any case the ratios of rates detected with muons to those detected with showers should be dependent on y for a given high energy neutrino flux.

5 Conclusions

The measurement of $\langle y \rangle$ at high energies in high energy neutrino interactions would give direct information on the behavior of the sea quarks distribution functions in the nucleon in a kinematic range unreachable to the most powerful accelerators, independently of the neutrino flux. We have presented a simple analytical parametrization which relates $\langle y \rangle$ with λ, the x slope of F_2 at low x and high Q^2.

We have also pointed out that neutrino telescopes are sensitive to the value of $\langle y \rangle$ and the possibility to measure y from the interference pattern of the radio-signals of the showers produced in the neutrino interaction.

Some other interesting information can be obtained from the measurement of y. For example, it has been proposed that supersymmetric effects, as R-parity violation could increase $\langle y \rangle$ with energy significantly [25]. Also the effect of extra dimensions in neutrino-nucleon interactions [26] should be manifested through the modification of $\langle y \rangle$ [27].

Acknowledgements

This work was supported by Xunta de Galicia under grant PGIDT00PXI20615PR and CICYT under grant AEN99-0589-C02-02).

References

[1] T.K. Gaisser, F. Halzen, and T. Stanev, Phys. Rep. **258** (1995) 173; P. Bhattacharjee and G. Sigl Phys. Rep. 327 (3-4) (2000) 109.

[2] F. Halzen et al, Proc. of the 24th Int. Cosmic Ray Conference (ICRC), Rome 1995.

[3] K. S. Capelle, J. W. Cronin, G. Parente and E. Zas, Astropart. Phys. **8** (1998) 321 [astro-ph/9801313].

[4] A. V. Butkevich, L. G. Dedenko, S. K. Karaevsky, A. A. Mironovich, A. L. Provorov and I. M. Zheleznykh, Phys. Part. Nucl. **29** (1998) 266.

[5] J. Alvarez-Muñiz, R. A. Vázquez, E. Zas Phys.Rev. D61 (2000) 023001

[6] V.N. Gribov and L.N. Lipatov, *Sov. J. Nucl. Phys.* **18** (1972) 438, 675;
L.N. Lipatov, *Sov. J. Nucl. Phys.* **20** (1975) 93;
G. Altarelli and G. Parisi, *Nucl.Phys.* **B126**, 298 (1977);
Yu.L. Dokshitzer, *Sov. Phys. JETP* **46** (1977) 641.

[7] A. M. Cooper-Sarkar, R. C. E. Devenish and A. De Roeck, *Int.J.Mod.Phys.* **A13** (1998) 3385.

[8] L.N. Lipatov, *Sov. J. Nucl. Phys.* **23** (1976) 642;
E.A. Kuraev, L.N. Lipatov and V.S. Fadin, *Sov. Phys. JETP* **44** (1976) 45; **45** (1977) 199;
Ya.Ya. Balitzki and L.N. Lipatov, *Sov. J. Nucl. Phys.* **28** (1978) 822;
L.N. Lipatov, *Sov. Phys. JETP* **63** (1986) 904.

[9] S. J. Brodsky, V. S. Fadin, V. T. Kim, L. N. Lipatov and G. B. Pivovarov, JETP Lett. **70** (1999) 155.

[10] A. De Rújula et al., Phys. Rev. **D10** (1974) 1649

[11] A. V. Kotikov and G. Parente, Nucl. Phys. **B549** (1999) 242

[12] G. Parente and E. Zas, Proc. of the 24th Int. Cosmic Ray Conference (ICRC), Rome 1995.

[13] Yu.M. Andreev, V.S. Berezinsky and A.Yu. Smirnov, Phys. Lett. B **84**, 247 (1979).

[14] A. Halprin and R. J. Oakes, FERMILAB-CONF-79/15-THY *Proc. of DUMAND Workshop, La Jolla, Calif., Jul 24 - Sep 2, 1978.*

[15] A.J. Buras, Rev. of Mod. Phys. 52, (1980) 1999.

[16] J. Kwiecinski, A.D. Martin, A.M. Stasto. Phys. Rev. D **56**, 3991 (1997).

[17] M. Glück, S. Kretzer, E. Reya Astropart. Phys. **11**, 327 (1999).

[18] R. Gandhi, C. Quigg, M.H. Reno, I. Sarcevic, Astropart. Phys. **5**, 81 (1996); Phys. Rev. D **58**, 093009 (1998).

[19] J. Kwiecinski, A.D. Martin, A.M. Stasto. Phys. Rev. D **59**, 093002 (1999).

[20] J.A. Castro-Pena, G. Parente and E. Zas, work in preparation.

[21] A.D. Martin, R.G. Roberts, W.J. Stirling and R.S Thorne, Eur. Phys. J. C4 (1998) 463.

[22] M. Gluck, E. Reya and A. Vogt, Eur. Phys. J. **C5** (1998) 461

[23] The IceCube NSF proposal http://pehno.physics.wisc.edu/icecube

[24] L. Landau and I. Pomeranchuk, Dokl. Akad. Nauk SSSR **92** (1953) 535; **92** (1935) 735; A.B. Migdal, Phys. Rev. **103** (1956) 1811; Zh. Eksp. Teor. Fiz. **32** (1957) 633 [Sov. Phys. JETP 5 (1957) 527].

[25] M. Carena, D. Choudhury, S. Lola and C. Quigg, Phys. Rev. **D58** (1998) 095003

[26] P. Jain, D. W. McKay, S. Panda and J. P. Ralston, Phys. Lett. **B484** (2000) 267

[27] M. Kachelrieβ and M. Plümacher, Phys. Rev. **D62** (2000) 103006

Figure captions

Figure 1. The total neutrino-nucleon deep inelastic cross section as a function of neutrino energy in lab frame for a) NC and CC neutrino and antineutrino interactions with MRST98 partons and b) CC neutrino interactions with MRST98 and GRV98 parton densities.

Figure 2. The average inelasticity y in deep inelastic neutrino-nucleon interaction as a function of laboratory neutrino energy for a) NC and CC neutrino and antineutrino interactions with MRST98 partons and b) CC neutrino interaction with MRST98 and GRV98 parton densities.

Figure 3. The parameter λ ($F_2 \sim x^{-\lambda}$) at low x and high $Q^2 \simeq M_W^2$ as a function of the average inelasticity in CC νN deep inelastic interaction.

Figure 4. a) The average Q^2 in deep inelastic CC neutrino-nucleon interaction as a function of the laboratory neutrino energy. b) The average x in deep inelastic CC neutrino-nucleon interaction as a function of the laboratory neutrino energy.

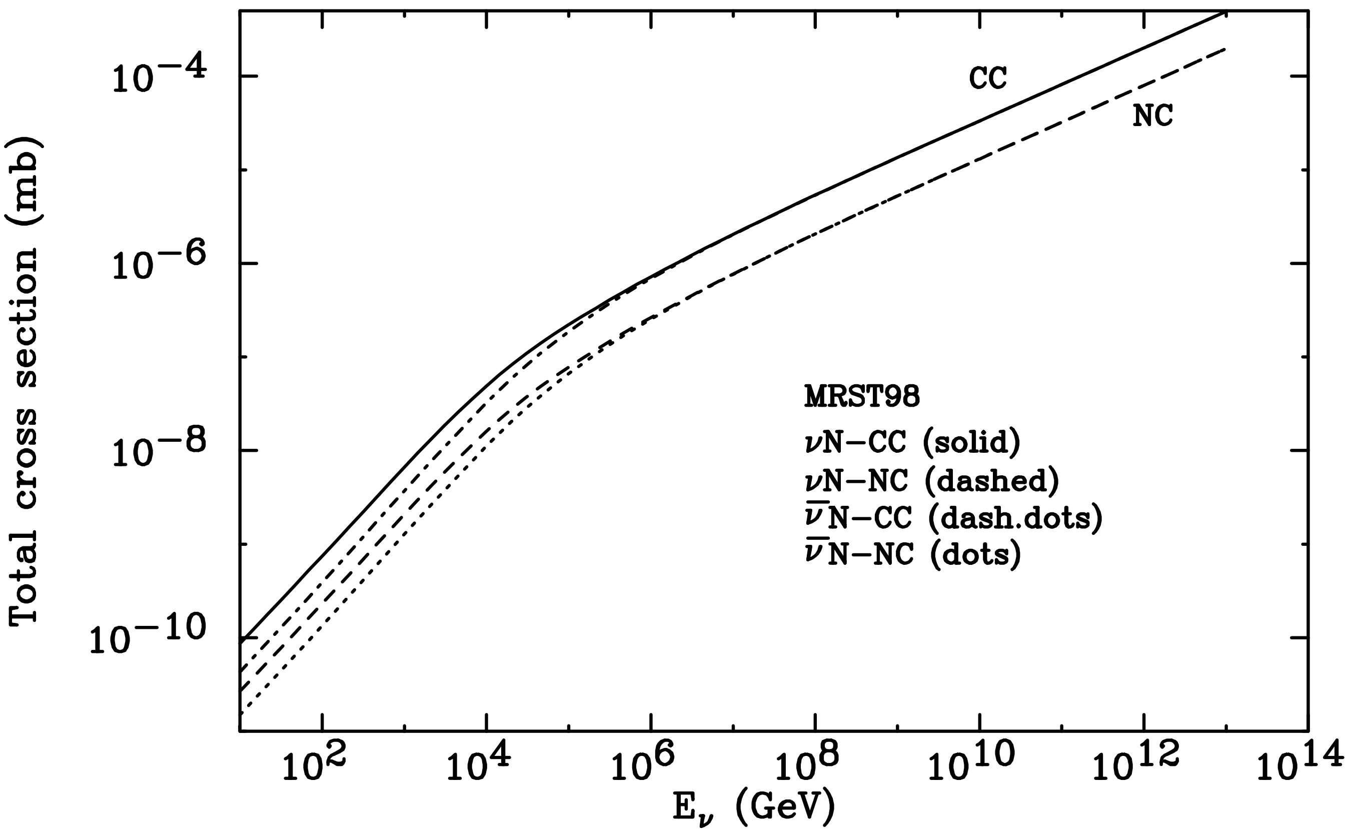

CC
NC
MRST98
νN−CC (solid)
νN−NC (dashed)
$\bar{\nu}$N−CC (dash.dots)
$\bar{\nu}$N−NC (dots)
Total cross section (mb)
10^{-4}
10^{-6}
10^{-8}
10^{-10}
10^{2}
10^{4}
10^{6}
10^{8}
10^{10}
10^{12}
10^{14}
E_ν (GeV)

Fig. 1a

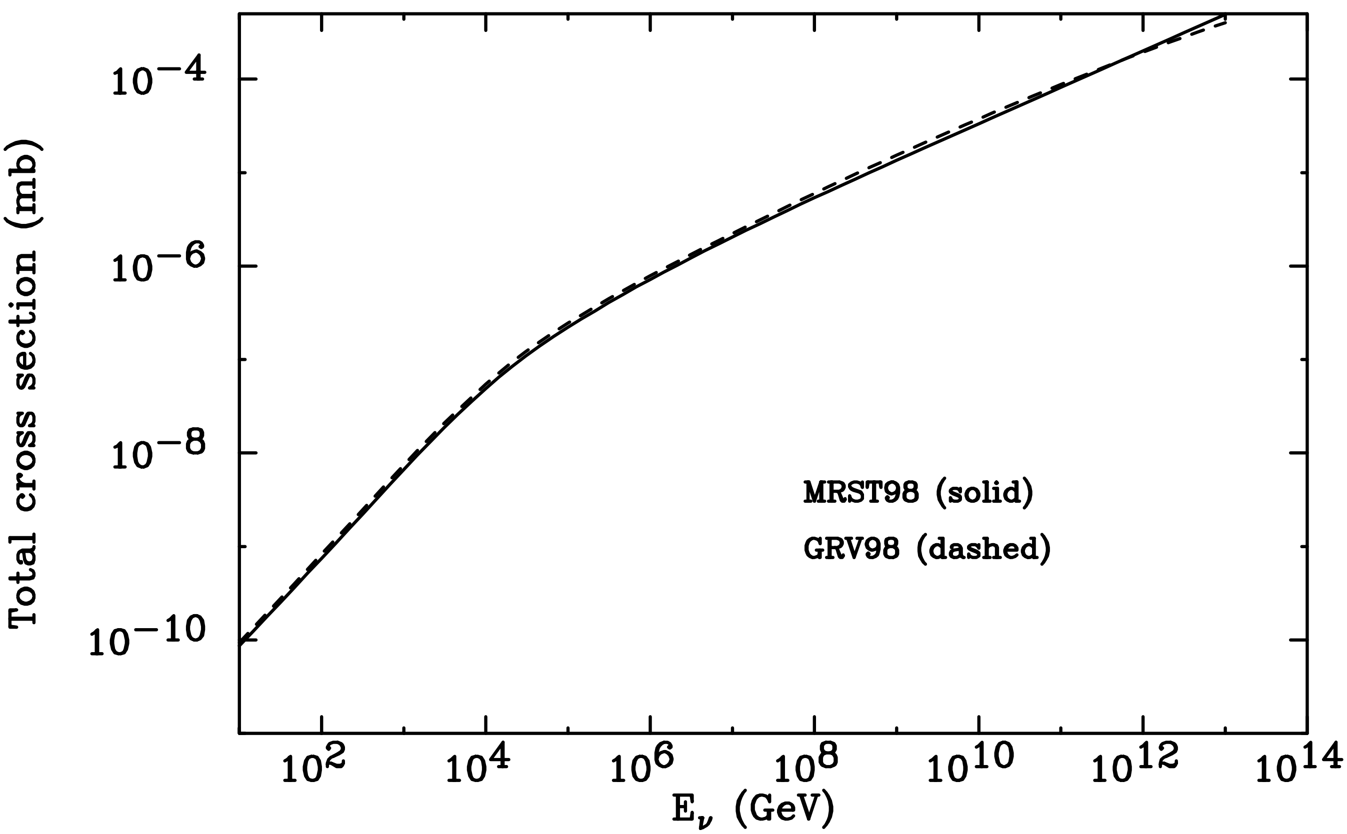

Total cross section (mb)
10^{-4}
10^{-6}
10^{-8}
10^{-10}
MRST98 (solid)
GRV98 (dashed)
10^{2}
10^{4}
10^{6}
10^{8}
10^{10}
10^{12}
10^{14}
E_ν (GeV)

Fig. 1b

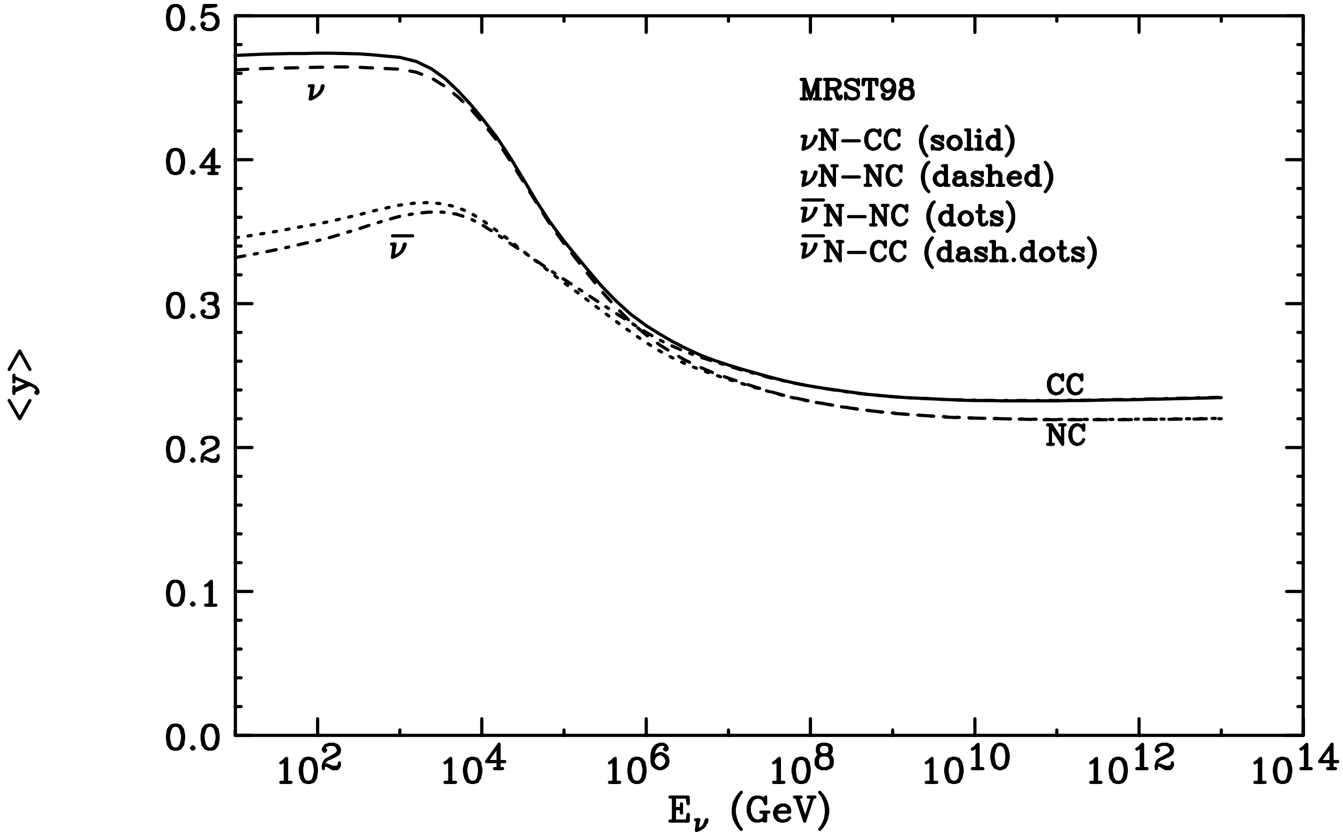

MRST98
νN−CC (solid)
νN−NC (dashed)
$\bar{\nu}$N−NC (dots)
$\bar{\nu}$N−CC (dash.dots)
ν
$\bar{\nu}$
CC
NC
0.0
0.1
0.2
0.3
0.4
0.5
<y>
10^2
10^4
10^6
10^8
10^{10}
10^{12}
10^{14}
E_ν (GeV)

Fig. 2a

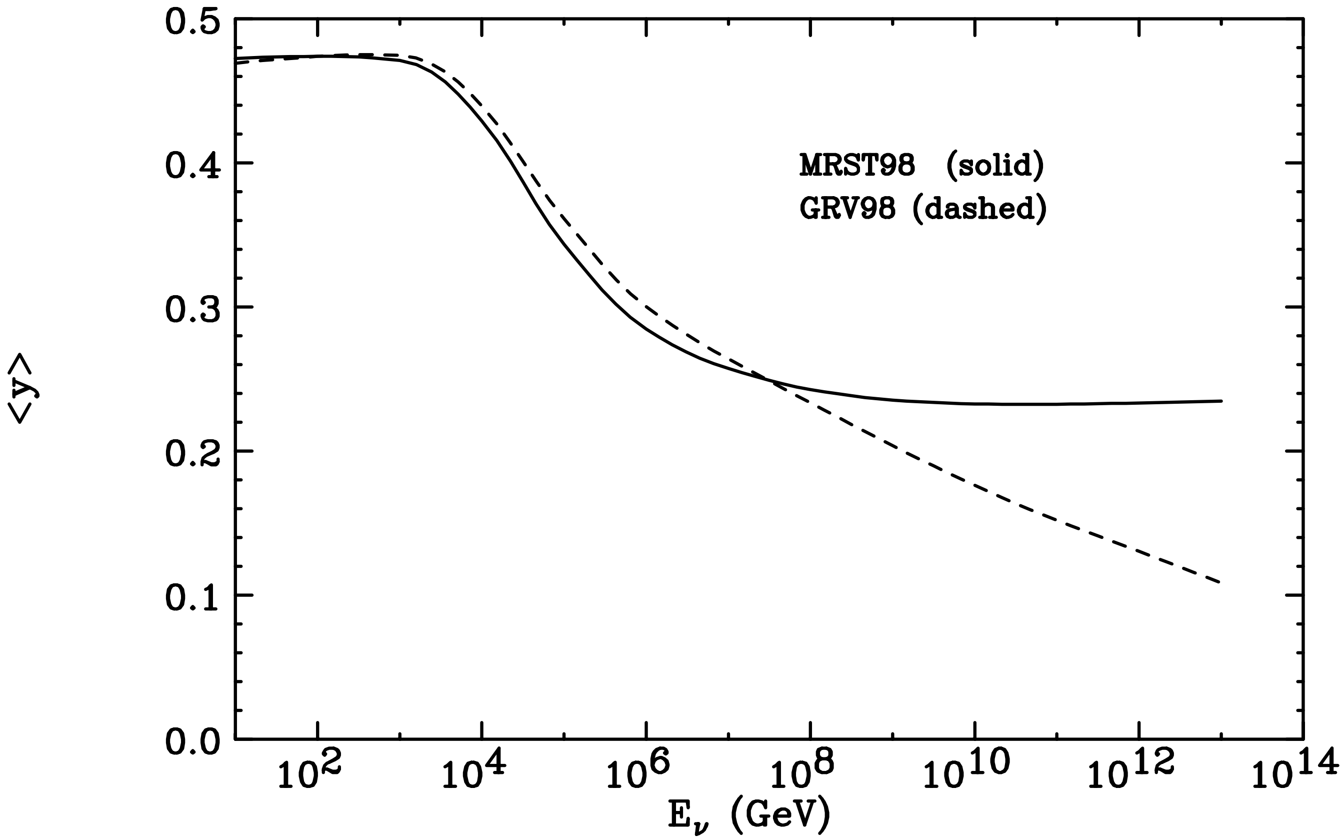
0.5
0.4
0.3
0.2
0.1
0.0
<y>
MRST98 (solid)
GRV98 (dashed)
10^2
10^4
10^6
10^8
10^{10}
10^{12}
10^{14}
E_ν (GeV)

Fig. 2b

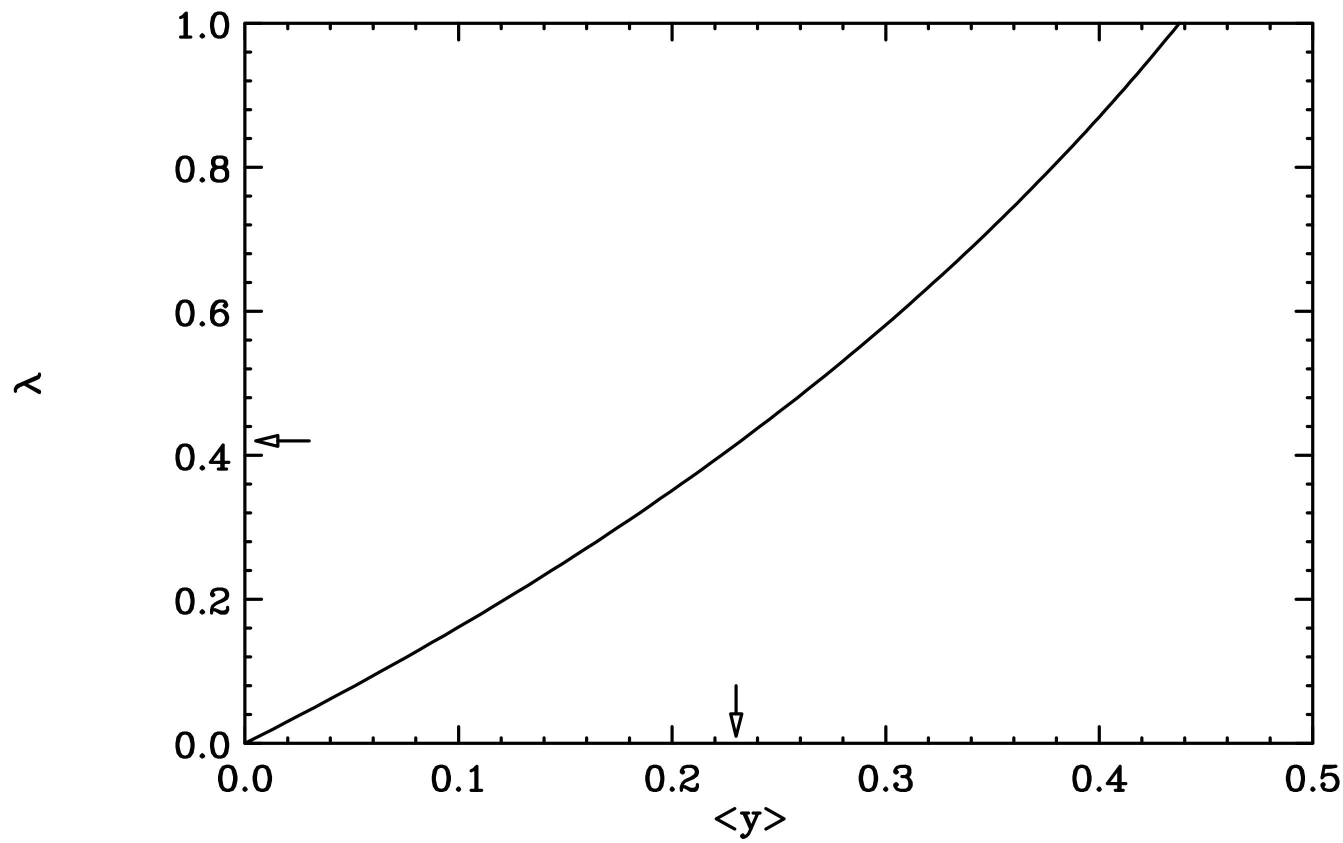

Fig. 3

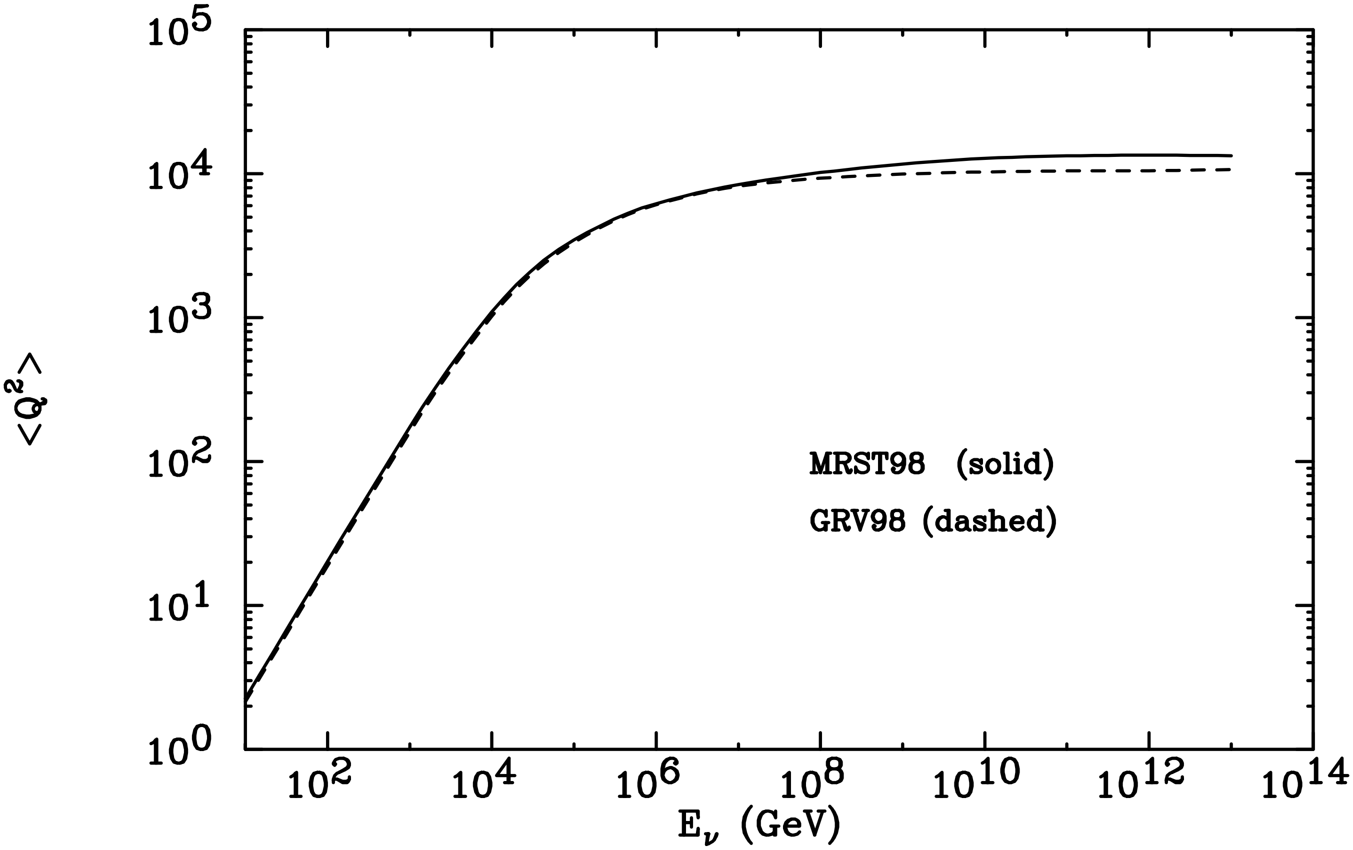

10^5
10^4
10^3
10^2
10^1
10^0
$<Q^2>$
MRST98 (solid)
GRV98 (dashed)
10^2
10^4
10^6
10^8
10^{10}
10^{12}
10^{14}
E_ν (GeV)

Fig. 4a

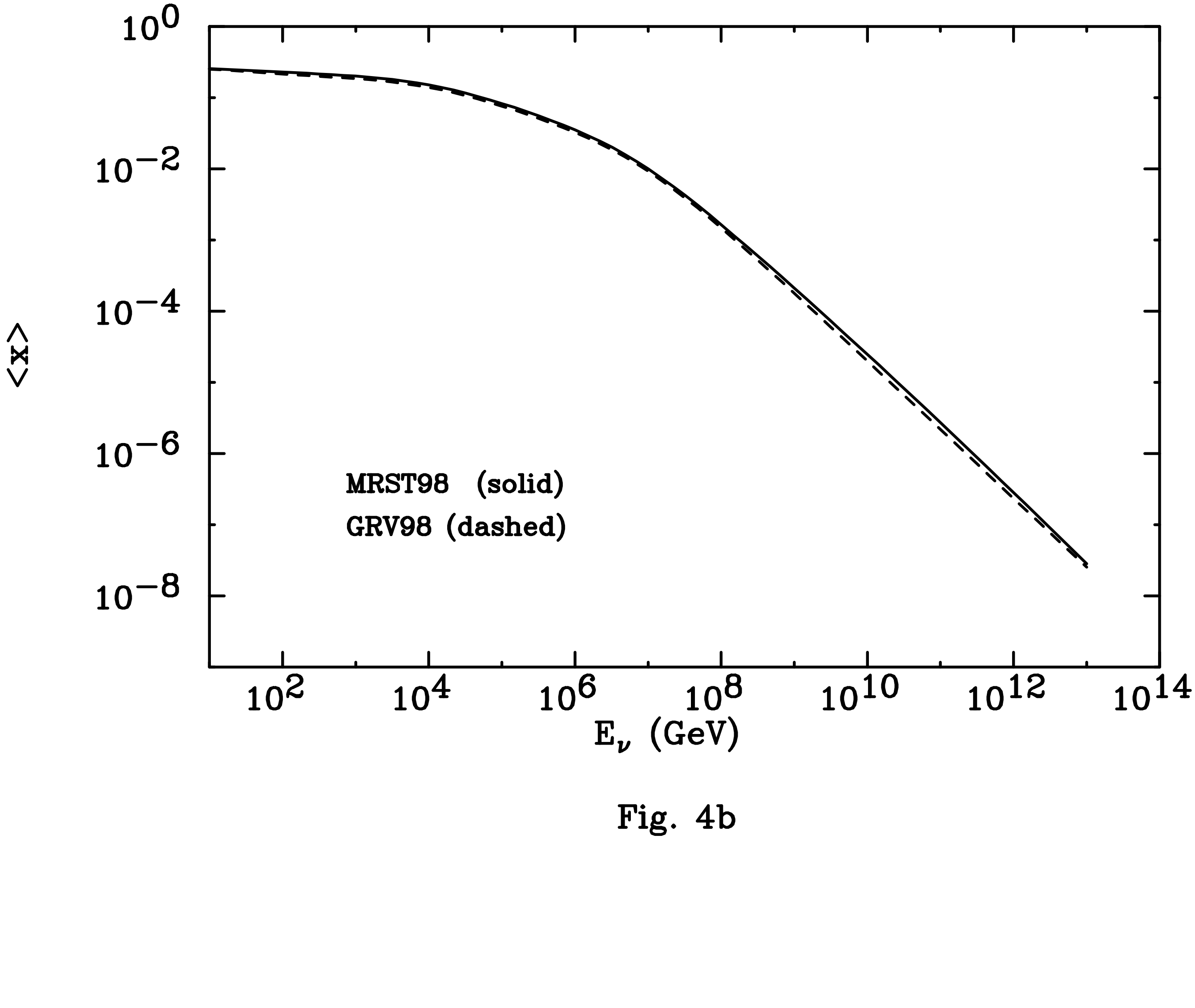

10^0
10^{-2}
10^{-4}
10^{-6}
10^{-8}
<x>
MRST98 (solid)
GRV98 (dashed)
10^2
10^4
10^6
10^8
10^{10}
10^{12}
10^{14}
E_ν (GeV)

Fig. 4b